

## Dehydrogenation Activity of Nickel-Tin-Silica Catalyst

MITSUO MASAI, KENJI MORI,<sup>1</sup> HIDEAKI MURAMOTO,<sup>2</sup>  
TAKASHI FUJIWARA<sup>3</sup> AND SHINJI OHNAKA

*Department of Chemical Engineering, Faculty of Engineering,  
Kobe University, Rokkodai-cho, Nada-ku, Kobe, Japan*

Received February 11, 1974; revised December 10, 1974

The effect of nickel-to-tin ratio on the following dehydrogenation reactions is studied, namely, cyclohexanone to phenol, cyclohexylamine to aniline, cyclohexane to benzene and 2-propanol to acetone. The optimum ratio catalyst for each reaction was Ni/Sn = 2.5 (atomic ratio), 8, 10 and 8, respectively. The rate of each reaction was zero order with respect to the partial pressure of reactant for cyclohexanone and 2-propanol, and first order for others. Metallic nickel and  $\beta$ -tin were observed on the catalysts by means of X-ray diffractometry. The presence of the alloy phases, such as Ni<sub>3</sub>Sn<sub>4</sub>, Ni<sub>3</sub>Sn<sub>2</sub> and NiSn, on the catalysts was also inferred on the basis of X-ray diffraction study on nickel-tin sintered metal. The presence of molten tin on the catalyst above about 230°C was proved by differential thermal analysis. Intimate contact of nickel and molten tin probably results in the formation of alloy phases without difficulty. The effect of the addition of tin seems to moderate the strong adsorption of polar substances on nickel-silica catalyst.

### INTRODUCTION

The dehydrogenation reaction of cyclohexanone and cyclohexanol to phenol on nickel-tin-silica catalyst has been reported by Swift and Bozik (1). According to them, catalyst of Ni/Sn = 2.5 (atomic ratio) has shown maximum selectivity and activity over the range of atomic ratio 0.9-4.5. They observed NiSn phase only on the catalyst of Ni/Sn = 0.9 which showed only a little activity, and they discussed the results mainly on the basis of this alloy formation. On the other hand, the phase diagram of nickel-tin systems is complex (2, 3). Three narrow range phases are present in the nickel-tin system according to handbooks (2,3). Therefore it is reasonable to suppose about this catalyst system that

other optimum nickel-to-tin ratios will be observed for other dehydrogenation reactions.

In the present work, the activity of nickel-tin-silica catalyst is studied extensively on the dehydrogenation reaction of cyclohexanone, cyclohexylamine, cyclohexane and 2-propanol. The catalyst of the maximum activity was different in nickel-to-tin ratio for each reaction. The orders of the dehydrogenation reaction rate were zero for oxygen-containing reactants and first for others. Presence of nickel,  $\beta$ -tin and alloy phases on the catalysts was indicated by means of X-ray diffractometry. It is shown by the comparison of the activity of nickel-tin-silica with that of nickel-silica that the addition of tin modifies the activity of nickel-silica to be sufficient for the dehydrogenation of polar compounds. This modification most likely results from the presence of mixed alloy phases on the surface of nickel crystallite, the presence of molten tin on the catalyst certainly leads

<sup>1</sup> Present address: Japan Gasoline Co. Ltd., Bessho-cho, Minami-ku, Yokohama, Japan.

<sup>2</sup> Present address: Sumitomo Chemical Engineering Co. Ltd., Hongo-3, Bunkyo-ku, Japan.

<sup>3</sup> Present address: Yanagimoto Mfg. Co. Ltd., Shimotoba, Fushimi-ku, Kyoto, Japan.

to the formation of these alloy phases during the reduction procedure of catalyst and during the reaction experiment above melting point of tin.

### METHODS

Nine catalysts were prepared by soaking silica hydrogel in the solution of both metal salts. The hydrogel was prepared by precipitation from the solution of sodium silicate at pH 8, and sodium ion was washed out almost completely. The soaking solution was practically a suspension of nickel nitrate hexahydrate and stannous chloride dihydrate mixed in known amount. After 24 hr soaking under intermittent but sufficient agitation, the soaking solution was evaporated. The dried hydrogel containing the salts of both metals was calcined at 500°C, 4 hr in the flow of air, and reduced at 500°C, 3 hr in the flow of hydrogen. The reduced catalyst was passivated carefully in very small partial pressure of oxygen in nitrogen atmosphere at room temperature just after reduction. Analytical values of catalysts prepared are shown in Table 1, these values were determined by chemical analysis. Values of the surface area of catalysts are contained also in Table 1, these were measured by the BET method using nitrogen as adsorbent.

To concentrate the metallic species on

TABLE I  
COMPOSITION AND SURFACE AREA OF CATALYSTS

Ni/Sn (atomic ratio)	Analytical data (mg/100 mg)		Surface area (m <sup>2</sup> /g)
	Ni	Sn	
0	0	10.7	
1	3.4	7.3	183
2.5	5.7	4.9	207
4.5	7.0	3.4	194
8	8.5	2.1	198
10	9.1	1.6	
∞	11.2	0	217
SiO <sub>2</sub>			241

the catalyst for the purpose of detailed X-ray diffraction study, nickel-tin sintered samples were prepared according to following procedures. Nickel carbonate and stannic oxide, both in fine powders, were mixed together. The mixture was shaped into a pellet under the pressure of 150 kg/cm<sup>2</sup>. Three pellets were prepared differing in nickel-to-tin atomic ratio, i.e., 1, 2.5 and 10. The calcination, reduction and passivation of these pellets were the same as those for the catalysts.

X-Ray diffraction patterns of calcined and reduced catalysts and of sintered samples were obtained by use of a Rigaku-Denki model D-3F diffractometer using Ni-filtered Cu-K $\alpha$  radiation, and the slit of the diffractometer was 0.1 mm in width.

The differential thermal analysis of the passivated catalyst was performed by use of a Shimadzu model MDB-10 differential thermal analyzer. Temperature was raised in the rate of 20°C/min, setting the sensitivity at 25  $\mu$ V.  $\alpha$ -Alumina was used as the reference material. The analysis was performed in hydrogen atmosphere of about 10<sup>-1</sup> Torr.

Reaction experiments were performed under atmospheric pressure using a conventional fixed bed reactor of flow type,

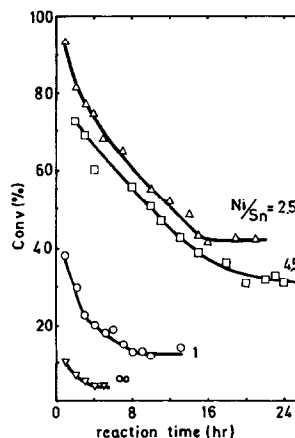


FIG. 1. Variation of the extent of conversion vs reaction time in the dehydrogenation of cyclohexanone at 400°C,  $W/F = 98$  g-cat·hr/g-mol reactant,  $H_2/C_6H_{10}O = 10$  (molar ratio).

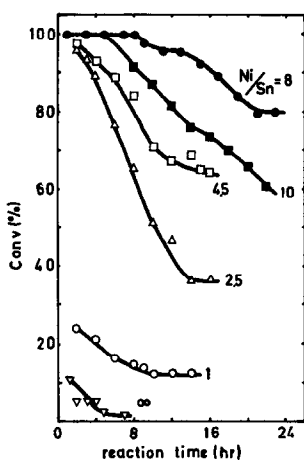


FIG. 2. Variation of the extent of conversion vs reaction time in the dehydrogenation of cyclohexylamine at 400°C,  $W/F = 96$  g-cat·hr/g-mol,  $H_2/C_6H_{11}NH_2 = 10$  (molar ratio).

which was made of 20 mm id Pyrex glass tube and was heated electrically from outside. Hydrogen was used as the carrier gas. The reactant was introduced to the reactor system by a syringe driven in constant rate. The detailed conditions for each reaction experiment are given in Figs. 1–4. Material in a trap at about 0°C, which was placed in the product stream of the reactor, was analyzed quantitatively using a gas chromatograph. The conditions for gas chromatographic analysis are shown in Table 2.

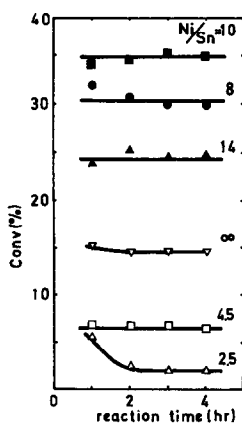


FIG. 3. Variation of the extent of conversion vs reaction time in the dehydrogenation of cyclohexane at 400°C,  $W/F = 31$  g-cat·hr/g-mol,  $H_2/C_6H_{12} = 7$  (molar ratio).

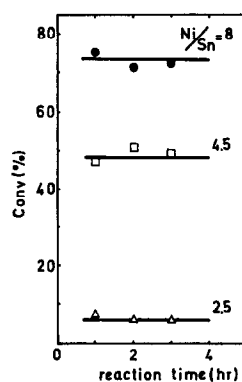


FIG. 4. Variation of the extent of conversion vs reaction time in the dehydrogenation of 2-propanol at 300°C,  $W/F = 20$  g-cat·hr/g-mol,  $H_2/C_3H_7OH = 5$  (molar ratio).

Mass balance was examined only on the catalyst, with which the maximum stationary activity was observed in each dehydrogenation reaction. Material in the product stream was condensed in a trap at 0°C, and weighed before the analysis. Flow rate of the stream from the trap which led to the sampling cock of a gas chromatograph was measured. Quantitative analysis was carried out by using a gas chromatograph which was calibrated to the weight of each material.

All the reagents were commercial GR grade. Gases were obtained commercially.

## RESULTS

Phenol was the major product in the dehydrogenation of cyclohexanone above 400°C. In this case, cyclohexene, benzene

TABLE 2  
THE CONDITIONS FOR GAS CHROMATOGRAPHY

Packed material in column (4 mm i.d. × 2 m)	Temp of column (°C)	Used in the dehydrogenation reaction of
Silicone DC550		
25 wt% on Celite	110	Cyclohexanone
Same as above	130	Cyclohexylamine
Same as above	60	Cyclohexane
Polyethylene glycol		
10 wt% on Diasolid-L	60	2-Propanol

and 2-(1-cyclohexenyl) cyclohexanone were observed as the minor products in low temperature range, i.e., 350–380°C, but their amount decreased with rising temperature and became quite negligible above 400°C. Aniline was the major product in the dehydrogenation of cyclohexylamine, and cyclohexene was the minor product. Benzene was formed in the dehydrogenation of cyclohexane. Acetone was the major product in the dehydrogenation of 2-propanol, and carbon monoxide, methane and methyl isobutyl ketone were observed as the minor products. On nickel-silica catalyst, carbon monoxide and methane were the major products in the dehydrogenation of 2-propanol. The tin-silica catalyst showed no activity on these reactions. The activity of the catalysts for each reaction is shown in Figs. 1–4. Variation of the extent of conversion of each reactant is plotted against the period of the reaction experiment in Figs. 1–4.

Mass balances of the dehydrogenation reactions were observed as follows. Cyclohexanone, 57.3 mol%; phenol, 40.9 mol%; benzene, 0.016 mol%; and cyclohexene, 0.00042 mol% were observed in the dehydrogenation of cyclohexanone on Ni/Sn = 2.5 at 400°C after 16 hr from the start of the reaction. Cyclohexylamine, 18.3 mol%; aniline, 79.0 mol%; and cyclohexene, 1.51 mol% were observed in the dehydrogenation of cyclohexylamine on Ni/Sn = 8 at 400°C after 21 hr from the start of reaction. Benzene was produced only in the dehydrogenation of cyclohexane on Ni/Sn = 10 in the period of reaction experiment shown in Fig. 4. 2-Propanol, 26.3 mol%; acetone, 72.1 mol%; methyl isobutyl ketone, 1.6 mol%; carbon monoxide, 0.001 mol%; and methane, 0.003 mol% were observed in the dehydrogenation of 2-propanol on Ni/Sn = 8 at 300°C after 2 hr from the start of the reaction. In the last reaction on nickel-silica, mass balance could not be

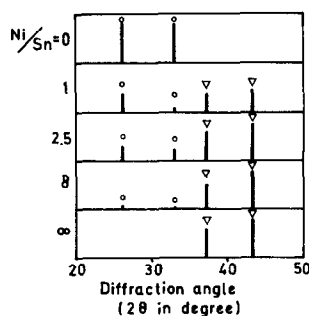


FIG. 5. X-Ray diffraction patterns of calcined catalysts, (○) SnO<sub>2</sub>, (▽) NiO.

examined because no stationary activity was observed.

Results of the kinetic study were as follows, zero order with respect to the partial pressure of cyclohexanone and of 2-propanol, while first order with respect to that of cyclohexylamine and of cyclohexane.

The X-ray diffraction patterns of the calcined and of the reduced catalysts are shown in Figs. 5 and 6, respectively. Oxides of both metals were observed on the calcined catalysts. Metallic nickel and  $\beta$ -tin were observed on the reduced catalysts. More detailed X-ray diffraction patterns were obtained about the metallic phases of these catalysts by sintered nickel-tin samples. These diffraction patterns are shown in Fig. 7. The observed phases are as follows: metallic nickel (4),  $\beta$ -tin (5), Ni<sub>3</sub>Sn<sub>4</sub> (6), Ni<sub>3</sub>Sn<sub>2</sub> (7) and NiSn (8). Though these X-ray diffraction patterns cannot be interpreted clearly, pres-

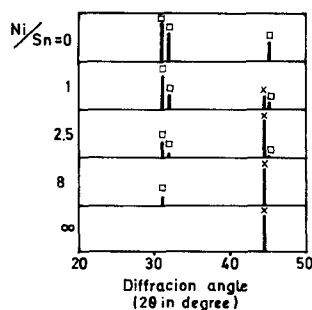


FIG. 6. X-Ray diffraction patterns of reduced catalysts, (□)  $\beta$ -Sn, (×) Ni.

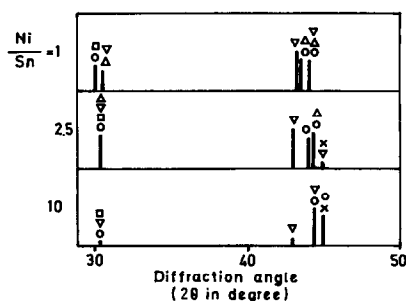


FIG. 7. X-Ray diffraction patterns of nickel-tin sintered metal: (x) Ni, (□)  $\beta$ -tin, (○)  $\text{Ni}_3\text{Sn}_4$ , ( $\Delta$ )  $\text{Ni}_3\text{Sn}_2$ , ( $\nabla$ ) NiSn.

ence of some alloy phases can be estimated as shown in Fig. 7. In Figs. 5–7, peak heights are shown in relative values to the highest peak of every chart. As shown in Fig. 8, the thermograms of the catalysts clearly show an endothermic peak at about 230°C. This endothermic peak can be ascribed to the melting of  $\beta$ -tin.

#### DISCUSSION

As Figs. 1–4 show, the addition of tin to nickel-silica catalyst clearly promotes the

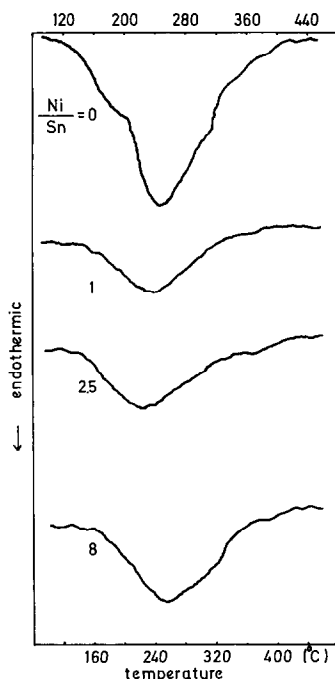


FIG. 8. Thermograms of the catalysts.

catalytic activity for these dehydrogenation reactions. It is noteworthy that the optimum nickel-to-tin ratio of the catalyst differs for each reaction, i.e.,  $\text{Ni}/\text{Sn} = 2.5$  for the dehydrogenation of cyclohexanone, 8 for cyclohexylamine, 10 for cyclohexane, and 8 for 2-propanol, respectively. The optimum ratio catalyst for the dehydrogenation of cyclohexanone has the same nickel-to-tin ratio as reported by Swift and Bozik (1). It is also noteworthy that the nickel-silica catalyst showed the highest activity for the reaction of 2-propanol; i.e., as the by-products of the reaction, methane, carbon monoxide and methyl isobutyl ketone were also observed in addition to acetone. Therefore, the role of tin is inferred to promote the dehydrogenation activity of nickel. Swift and Bozik have proposed that this modification of activity arises from the filling of 3d-band of nickel by the electrons from tin (1).

The state of both metals on the catalyst will be discussed at first. Metallic nickel and  $\beta$ -tin were observed on our reduced catalyst. Swift and Bozik observed only NiSn phase basing on the results of X-ray diffractometry on the catalyst of  $\text{Ni}/\text{Sn} = 0.9$ , while both free nickel and NiSn phase on the catalyst of  $\text{Ni}/\text{Sn} = 2.5$  and 4.5 (1). In both the present and their work, the catalysts of  $\text{Ni}/\text{Sn} = 1$  or 0.9 showed only a little activity on the dehydrogenation of cyclohexanone. Hence, it is reasonable to infer NiSn phase to be of low activity. On the other hand, NiSn phase was not observed in our catalysts as shown in Fig. 6. This discrepancy may arise from the low concentration of metallic phases in our catalysts. Therefore sintered nickel-tin metals were prepared to make the metallic phases concentrate. As Fig. 7 shows, the X-ray diffraction patterns of these sintered metals give no clear assignment of each diffraction peak obtained. However, these X-ray diffraction patterns indicate the presence of different phases; i.e., (a)  $\text{Ni}_3\text{Sn}_4$ ,  $\text{Ni}_3\text{Sn}_2$ , NiSn and

$\beta$ -tin in Ni/Sn = 1, (b)  $\text{Ni}_3\text{Sn}_4$ ,  $\text{Ni}_3\text{Sn}_2$ , NiSn, nickel and  $\beta$ -tin in Ni/Sn = 2.5, and (c)  $\text{Ni}_3\text{Sn}_4$ , NiSn and nickel in Ni/Sn = 10. From these results, irrespective of the clear identification of each phase, it is probable to infer the presence of mixed and partially alloyed phases. These alloyed phases may be ascribed to such phases as  $\text{Ni}_3\text{Sn}_4$ ,  $\text{Ni}_3\text{Sn}_2$ , and NiSn, lying on the interface between nickel and tin. This shows that the formation of a complete alloy phase cannot be expected. Then, it seems probable to infer the presence of metallic nickel,  $\beta$ -tin and some alloy phases on the catalysts. The differential thermal analysis of the catalysts showed the presence of  $\beta$ -tin phase also (Fig. 8). This agrees with the results described above.

Now, let us discuss the metallic phases on the catalysts further. Three miscibility gaps are accepted in recent handbooks (2, 3), i.e., Ni<sub>3</sub>Sn, Ni<sub>3</sub>Sn<sub>2</sub> and Ni<sub>3</sub>Sn<sub>4</sub>. The temperatures of the formation are 1174°C for Ni<sub>3</sub>Sn and 1264°C for Ni<sub>3</sub>Sn<sub>2</sub>, respectively, while Ni<sub>3</sub>Sn<sub>4</sub> is formed by peritectic reaction between Ni<sub>3</sub>Sn<sub>2</sub> and liquid at 795°C (2).<sup>4</sup> Our catalysts were reduced at 500°C which is considerably lower than the above temperatures. Therefore, under this reduction temperature, nickel may not melt but rather may dissolve into molten tin which is present abundantly on the catalyst. On the other hand, nickel is practically insoluble in tin, i.e., about 3 at.% at 500°C (2). Hence, nickel appears to be precipitated from the solution when cooled. During the reduction of catalyst, a nickel crystallite is surrounded by molten tin closely. Tin will diffuse into nickel crystallite, and this diffusion results in the formation of alloy phases. On the other hand, Sachtler and Van der Plank (9) pro-

posed about nickel-copper catalyst, in which no molten metal is present at the condition of normal treatment, that the formation of alloy phases proceeds through the interdiffusion of the atoms of two metals. In our case, one of two metals is in molten state as shown in Fig. 8, the contact of two metals should be closer than nickel-copper system. Therefore, the diffusion of tin into nickel is presumably smoother than the interdiffusion of nickel-copper system. These discussions may explain the formation of mixed and partly alloyed phases on the surface of nickel crystallite.

The rate of the dehydrogenation of cyclohexanone and that of 2-propanol were of zero order to the partial pressure of the reactant. These results indicate the strong adsorption of two reactants if the Langmuir-Hinshelwood type kinetic equation is assumed. The strong adsorption of oxygen-containing substances such as acetone and 2-propanol on nickel catalyst is indicated by the fact that 2-propanol was converted to carbon monoxide, methane and methyl isobutyl ketone in addition to acetone on nickel-silica. A part of these strongly adsorbed substances may be decomposed to carbon monoxide and methane which can leave the catalyst easily, while the other part which cannot leave the catalyst by such decomposition may become poisons on the catalyst. Thus, the activity of nickel-silica on the dehydrogenation of cyclohexanone is quite low as shown in Fig. 1. This strong adsorption may also retard the activity of nickel-silica for cyclohexylamine as shown in Fig. 2. In support of this discussion, cyclohexane which is a substance of low polarity reacted considerably on nickel-silica, as shown in Fig. 3. These results indicate that nickel-silica is not suitable to make polar substances react, because of the poisonous effect mentioned above. Hence, the role of tin is concluded to weaken the strong adsorption of polar substances. This role of

<sup>4</sup> NiSn is replaced by Ni<sub>3</sub>Sn<sub>4</sub> in the handbook. ASTM Powder Diffraction Cards present different X-ray diffraction pattern for Ni<sub>3</sub>Sn<sub>4</sub> (6) and NiSn (8), we cannot decide whether NiSn phase is actually present or not. We believe the data shown in Fig. 7 and the results of Swift and Bozik (1).

tin is inferred to arise from the gradual filling of 3d-band of nickel by the electrons from tin. It may be concluded, therefore, that the surface alloy on nickel crystallite, which make the electron interaction sure, is responsible for catalytic activity. The shift of the nickel-to-tin ratio of the catalyst of optimum activity may arise from the difference in the degree of the mixing of both metals in surface alloy.

#### ACKNOWLEDGMENTS

The authors express their thanks to Professor Kozo Hirota of Chiba Institute of Technology (Professor Emeritus of Osaka University) for helpful discussions and encouragement relating to this work,

and also to Mr. Kenji Nomura for his cooperation in the experiments.

#### REFERENCES

1. Swift, H. E., and Bozik, J. E., *J. Catal.* **12**, 5 (1968).
2. Hansen, M., and Anderko, K., "Constitution of Binary Alloys" 2nd ed., p. 1042. McGraw-Hill, New York, 1958.
3. Shunk, F. A., "Constitution of Binary Alloys," 2nd Suppl., p. 555. McGraw-Hill, New York, 1969.
4. ASTM Powder Diffraction Cards, 4-0850.
5. ASTM Powder Diffraction Cards, 4-0673.
6. ASTM Powder Diffraction Cards, 4-0845.
7. ASTM Powder Diffraction Cards, 6-0414.
8. ASTM Powder Diffraction Cards, 3-1004.
9. Sachtler, W. M. H., and Van der Plank, P., *Surface Sci.* **18**, 62 (1969).